

AD-A197 458

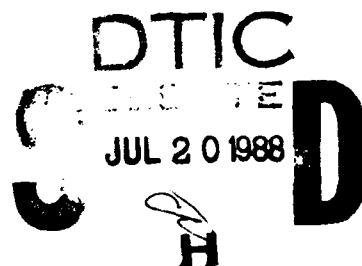
AD

TECHNICAL REPORT ARCCB-TR-88019

PREMARTENSITE TRANSFORMATION IN $Ni_{50.5}Ti_{49.5}$

L. V. MEISEL

P. J. COTE



APRIL 1988



**US ARMY ARMAMENT RESEARCH,
DEVELOPMENT AND ENGINEERING CENTER
CLOSE COMBAT ARMAMENTS CENTER
BENÉT LABORATORIES
WATERVLIET, N.Y. 12189-4050**



APPROVED FOR PUBLIC RELEASE; DISTRIBUTION UNLIMITED

DISCLAIMER

The findings in this report are not to be construed as an official Department of the Army position unless so designated by other authorized documents.

The use of trade name(s) and/or manufacturer(s) does not constitute an official indorsement or approval.

DESTRUCTION NOTICE

For classified documents, follow the procedures in DoD 5200.22-M, Industrial Security Manual, Section II-19 or DoD 5200.1-R, Information Security Program Regulation, Chapter IX.

For unclassified, limited documents, destroy by any method that will prevent disclosure of contents or reconstruction of the document.

For unclassified, unlimited documents, destroy when the report is no longer needed. Do not return it to the originator.

REPORT DOCUMENTATION PAGE		READ INSTRUCTIONS BEFORE COMPLETING FORM
1. REPORT NUMBER ARCCB-TR-88019	2. GOVT ACCESSION NO. ADA197458	3. RECIPIENT'S CATALOG NUMBER
4. TITLE (and Subtitle) PREMARTENSITE TRANSFORMATION IN $Ni_{50.5}Ti_{49.5}$		5. TYPE OF REPORT & PERIOD COVERED Final
7. AUTHOR(s) L. V. Meisel and P. J. Cote		6. PERFORMING ORG. REPORT NUMBER
9. PERFORMING ORGANIZATION NAME AND ADDRESS US Army ARDEC Benet Laboratories, SMCAR-CCB-TL Watervliet, NY 12189-4050		8. CONTRACT OR GRANT NUMBER(s)
11. CONTROLLING OFFICE NAME AND ADDRESS US Army ARDEC Close Combat Armaments Center Picatinny Arsenal, NJ 07806-5000		10. PROGRAM ELEMENT, PROJECT, TASK AREA & WORK UNIT NUMBERS AMCMS No. 6111.02.H610.011 PRON No. 1A82Z8CANMSC
14. MONITORING AGENCY NAME & ADDRESS (if different from Controlling Office)		12. REPORT DATE April 1988
		13. NUMBER OF PAGES 19
		15. SECURITY CLASS. (of this report) UNCLASSIFIED
		15a. DECLASSIFICATION/DOWNGRADING SCHEDULE
16. DISTRIBUTION STATEMENT (of this Report) Approved for public release; distribution unlimited.		
17. DISTRIBUTION STATEMENT (of the abstract entered in Block 20, if different from Report)		
18. SUPPLEMENTARY NOTES Submitted to <u>Physical Review</u> (American Physics Society).		
19. KEY WORDS (Continue on reverse side if necessary and identify by block number) Shape Memory Alloys, Nickel Titanium Alloys, Nickel Alloys, Martensite Transformations, Differential Scanning Calorimetry . (fig 1) ←		
20. ABSTRACT (Continue on reverse side if necessary and identify by block number) Small deviations from stoichiometry in the thermoelastic NiTi martensitic alloy yield sufficiently large separation of the martensite and premartensite transformations to allow a thermal analysis study of the premartensite transformation without the complication of competing phenomena. The nature of the premartensite transformation in $Ni_{50.5}Ti_{49.5}$ and its relation to similar phenomena in stoichiometric and iron-doped NiTi is the subject of the present report. Data indicate that the premartensite transformation width in (CONT'D ON REVERSE)		

20. ABSTRACT (CONT'D)

cont'd → $\text{Ni}_{50.5}\text{Ti}_{49.5}$ is due to a distribution of regions of the sample that transform from the cubic to the rhombohedrally distorted CsCl phase over a range of temperatures, and these regions transform back to cubic CsCl structure in reverse order upon reheating. In contrast to the results in iron-doped NiTi, no evidence of a two-step transformation could be found in a series of studies of the metastability and transformation kinetics of mixtures of phases produced by partially transforming from the pure CsCl phase and from the pure rhombohedrally distorted CsCl phase. This lack of evidence may not be conclusive since the physical properties of the charge density wave state (on cubic CsCl lattice) and the rhombohedrally distorted CsCl may be similar; however, if these two phases exist in $\text{Ni}_{50.5}\text{Ti}_{49.5}$, then they must also have essentially identical ranges of temperature for metastability and identical transformation kinetics.

Kayman →

UNCLASSIFIED

TABLE OF CONTENTS

	<u>Page</u>
INTRODUCTION	1
EXPERIMENTAL DETAILS	4
RESULTS AND DISCUSSION	5
Continuous Cooling and Heating Curves	5
Interrupted Heating and Cooling DSC Runs	6
SUMMARY AND CONCLUSIONS	10
REFERENCES	13

LIST OF ILLUSTRATIONS

- | | |
|---|----|
| 1. Heat flow versus temperature for constant heating rates of 0.1, 0.2, 0.5, 1.0, and 2.0°C/minute in Ni _{50.5} Ti _{49.5} . Also shown are four (essentially) identical cooling runs obtained for a rate of -0.5°C/minute made between the heating runs. These curves and those shown in the subsequent figures are uncalibrated; to obtain true heat flow multiply a given value by 0.86. | 15 |
| 2. DSC results illustrating metastability and subsequent further transformation of mixtures of phases produced by interrupting the premartensite transformation in Ni _{50.5} Ti _{49.5} . Curves following 0 and 30-minute isothermal holds at 39.1°C are shown. Standard DSC curves are also shown. Heating and cooling rates were 0.1°C/minute. Isothermal holds greater than 8 minutes yield curves indistinguishable from the 30-minute case. | 16 |
| 3. DSC results illustrating metastability and reverse transformation of mixtures of phases produced by interrupting the premartensite transformation in Ni _{50.5} Ti _{49.5} . Curves following 0, 2, and 30-minute isothermal holds at 39.0°C are shown. Standard DSC curves are also shown. Heating and cooling rates were 0.1°C/minute. | 17 |
| 4. DSC results illustrating metastability and reverse transformation of mixtures of phases produced by interrupting the reverse premartensite transformation in Ni _{50.5} Ti _{49.5} . Curves following 0 and 30-minute isothermal holds at 40.9°C are shown. Standard DSC curves are also shown. Heating and cooling rates were 0.1°C/minute. Note the increased start temperature and initial reaction rate in the retained rhombohedrally distorted CsCl phase cases. | 18 |



For	
<input checked="" type="checkbox"/>	
<input type="checkbox"/>	
<input type="checkbox"/>	
Justification	
By	
Distribution/	
Availability Codes	
Dist	Avail and/or Special
A-1	

INTRODUCTION

Lattice instability and soft phonon modes have long been associated with martensite transformations (ref 1). For example, Testardi (ref 2) discussed the association of structural instabilities and superconductivity in A-15 alloys, in which the cubic to tetragonal (martensite) transformation is referred to as the Bitterman-Barrett (ref 3) transformation, and Nakanishi (ref 4) provides a similar discussion of lattice softening associated with martensite transformations with particular emphasis on thermoelastic martensite exhibiting shape memory effects.

The most dramatic observations of premartensitic phenomena showed that the relevant shear elastic constants approach zero as the temperature approaches the martensite start temperature (M_S). Delaey et al. (ref 5) have also pointed out that combinations of phonons having wave vectors and polarizations consistent with the martensite transformation become soft as M_S is approached.

Because of their commercial importance, NiTi alloys have been the subject of intensive study. Diffraction studies of Sandrock et al. (ref 6) have demonstrated that in stoichiometric NiTi, a diffuse (1,1,1) reflection appears at temperatures well above M_S , and a (5/3, 7/3, 0) reflection appears about 30°C above M_S . Moreover, while the (1,1,1) reflection remains relatively constant in intensity, the (5/3, 7/3, 0) intensity increases sharply as the temperature is reduced toward M_S , reaches a cusp-like maximum near M_S , and then decreases sharply below M_S , finally vanishing near the martensite finish temperature (M_f). Similar premartensitic effects are seen in thermal analysis and electrical resistivity studies in NiTi alloys and have been ascribed to instability effects in the parent phase (CsCl structure).

References are listed at the end of this report.

The close proximity of the premartensite transformation and the martensite transformation in temperature has made the study of the premartensite transformation in stoichiometric NiTi unwieldy. Recently, Matsumoto and Honma (ref 7) demonstrated that in $\text{Ti}_{50}\text{Ni}_{47}\text{Fe}_3$, an effective isolation of the premartensite transformation is possible. Salamon, Meichle, and Wayman (ref 8) (SMW) measured x-ray and neutron diffraction, specific heat, and magnetic susceptibility associated with the premartensite transformation in iron-doped NiTi alloys in which the martensite transformation is completely suppressed.

In the following discussion, the CsCl phase (parent phase) is denoted as β . Following SMW, let T_I be the temperature at which superlattice reflections first appear on cooling the β phase. T_I corresponds to the start temperature for the premartensite transformation as seen, for example, in a differential scanning calorimetry (DSC) study. Let T_f be the finish temperature for the premartensite transformation. The rhombohedrally distorted CsCl phase, which is metastable at temperatures between M_S and T_f , will be denoted as β' .

According to SMW, the premartensite transformation consists of two separate transformations: the first, which commences at T_I , yields a phase composed of incommensurate charge density waves on an undistorted cubic CsCl lattice. We denote this phase β^* . The β^* phase subsequently transforms to β' , by a "lock-in" transformation (wherein the host lattice distorts to accommodate the wave vector of the wave that produces the superlattice reflections) which commences at a temperature T_r . At this temperature SMW observe the abrupt appearance of Bragg peak splittings.

To summarize the SMW picture, one has the following metastable states for NiTi alloys cooled from above T_I :

1. $T > T_I$: Pure β phase.

2. $T_I > T > T_R$: Either pure β^* phase exists, in which the charge density wave (CDW) intensity increases as T approaches T_R , or mixtures of β and β^* phases coexist. In either case, the atomic arrangement remains (cubic) CsCl.

3. $T_R > T > T_f$: At T_R an abrupt lock-in occurs (Bragg peaks split), wherein the structure becomes β' , i.e., rhombohedrally distorted CsCl. As the temperature is reduced toward T_f , the rhombohedral angle increases continuously. SMW discuss this as though the crystal were 100 percent rhombohedrally distorted CsCl throughout this temperature range.

It may be possible to interpret the present data in terms of pure β^* with increasing CDW intensity for $T_I > T > T_R$ and pure β' with increasing rhombohedral angle for $T_R > T > T_f$ following SMW, but we will present our discussion allowing for mixtures of phases. Thus, for example, when we speak of metastable mixtures of phases, one might also consider a metastable rhombohedral angle or intensity for a CDW state.

4. $T_f > T > M_S$: Pure β' phase with invariant rhombohedral angle.

SMW made the following observations in their study of the premartensite transformation in 3.2 percent iron-doped NiTi: (1) $T_I = 232^\circ\text{K}$, (2) $T_R = 224^\circ\text{K}$, and (3) except for the observation of needle-shaped regions having a (1,1,0) twin relationship with surrounding material and the appearance of small shoulders on the (2,2,2), (2,2,0), and (2,1,0) Bragg peaks, no discontinuities are seen in any measurements as T passes through T_R . (SMW suggest that resistivity and specific heat anomalies occur at T_R ; however, it is evident from their Figures 2 and 4 that these effects commence near T_I and, in fact, the resistivity versus T curve and the (2/3,1/3,0) neutron superlattice peak intensity versus T curve have essentially the same shape.)

We report here on a thermal analysis study of the premartensite transformation in $\text{Ni}_{50.5}\text{Ti}_{49.5}$. As suggested by Nishida and Wayman (unpublished, as referenced in SMW), the premartensite transformation is well separated from the martensite transformation in this alloy ($T_f \approx 38^\circ\text{C}$, $M_s \approx 10^\circ\text{C}$). It is interesting that upon heating this alloy from the purely martensite phase, transformation to β' (or possibly β^*) is followed by transformation to β phase. We provide detailed information on the nature of the premartensite transformation in $\text{Ni}_{50.5}\text{Ti}_{49.5}$ and, in particular, address the proposal of SMW that there are actually two phase transformations ($\beta \rightarrow \beta^*$ and $\beta^* \rightarrow \beta'$) comprising the premartensite transformation in NiTi alloys.

EXPERIMENTAL DETAILS

All of the data were accumulated using a Dupont 1090 Thermal Analysis System. The data given in the figures were obtained from a disc-shaped sample of material whose mass is 33 mg. Equivalent results were obtained for other samples. The heat flow values shown in the figures are "uncalibrated." The Dupont 1090 system requires a temperature-dependent calibration. The calibration constant appropriate to the temperature range of the premartensite transformation in $\text{Ni}_{50.5}\text{Ti}_{49.5}$ was obtained via determination of the specific heat of aluminum and yields a value of 0.86 (i.e., true value = $0.86 \times$ measured value). The aluminum specific heat calibration is consistent with indium (and other) melting enthalpy calibrations. The samples were fabricated from material supplied by Reactive Metals, Inc., which was the subject of an earlier study by Milligan (ref 9).

All DSC data presented were preceded by an isothermal soak at a temperature near the transformation range (either in pure β or pure β' phase) for several

hours. When this stage was omitted, characteristic temperatures varied during the course of an experiment by up to 0.4°C.

RESULTS AND DISCUSSION

Continuous Cooling and Heating Curves

The samples in these runs were prepared in pure β phase to obtain continuous cooling curves and in pure β' phase to obtain continuous heating curves. The continuous cooling transformations began at $39.8 \pm 0.1^\circ\text{C}$ (i.e., $T_I \approx 39.8^\circ\text{C}$). Figure 1 shows DSC results following a four-hour isothermal hold at 39°C for heating rates of 0.1, 0.2, 0.5, 1.0, and 2.0°C/minute . Also shown are four essentially identical cooling curves obtained at $-0.5^\circ\text{C/minute}$. The identical cooling rates between the varying heating rates were employed to confirm the absence of drifts in the DSC apparatus and the absence of significant changes in the sample. A set of cooling curves for different rates looks very similar to the set of heating curves shown; one may compare the $-0.5^\circ\text{C/minute}$ curve shown in Figure 1 with the curves for -0.1°C shown in the later figures. Transformation enthalpy deduced from these curves is $4.75 \pm 0.1 \text{ J/gm}$ (including the calibration correction); it is rate-independent and is equal to that obtained from cooling curves within experimental uncertainties. Compare this with 6.49 J/gm in $\text{Ni}_{50.5}\text{Ti}_{49.5}$ as measured by Mukherjee et al. (ref 10). Although the Dupont 1090 will not control for $|\dot{T}| < 0.1^\circ\text{C}$, it is clear from our determination of isothermal transformation effects described in the next subsection, that an even sharper transformation would be observed at lower rates.

Note that the premartensite DSC peaks observed in nonstoichiometric $\text{Ni}_{50.5}\text{Ti}_{49.5}$ at rates less than 2°C/minute are much sharper than those seen in stoichiometric NiTi at 10°C/minute and in 3.2 percent iron-doped NiTi alloys as

reported by SMW (for an unspecified cooling rate). Also, as reported by SMW for their iron-doped NiTi alloys, there is no indication in these (standard) DSC results of a two-step transformation process.

Interrupted Heating and Cooling DSC Runs

We performed a variety of experiments on samples prepared in mixtures of phases. The purpose of these studies was to obtain detailed information concerning the nature of the premartensite transformation and, in particular, to search for thermal evidence for a two-part transformation in which only $\beta + \beta^*$ mixtures occur for temperatures between T_I and T_R and mixtures of β' , β^* , and β occur for temperatures between T_R and T_f . Because the transformation peaks are very sharp, all the interrupted DSC curves shown were obtained for $|\dot{T}| = 0.1^\circ\text{C/minute}$ (the slowest rate controlled by the Dupont 1090 system).

Figure 2 exhibits a DSC run obtained by (1) holding at 44°C for 5 hours, (2) cooling to 39.1°C , (3) heating to 40°C , (4) cooling to 36°C , (5) heating to 44°C , (6) cooling to 39.1°C , (7) holding at 39.1°C for 30 minutes, (8) heating to 40°C , and (9) cooling to 36°C . The section of the DSC curve obtained following the 30-minute hold at 39.1°C is essentially identical to that for any isothermal hold longer than 8 minutes at 39.1°C . We shall refer to a DSC curve obtained by heating or cooling entirely through a transformation as a standard DSC curve, as opposed to curves obtained from interrupted transformations. The standard DSC curve obtained by cooling, starting from the pure β phase at 0.1°C/minute is also shown. The results in Figure 2 are qualitatively equivalent to runs obtained with interruptions throughout the entire cooling peak. These results show that: (1) No temperature of interruption exists between T_I and T_f where any qualitative change in the subsequent behavior of the mixture of

phases produced by the interrupted transformation could be found in a DSC study. In particular, for a given fraction transformed (whether during a 30-minute isothermal hold at a given temperature or a 30-second isothermal hold at a lower temperature) identical subsequent behavior is observed in these DSC studies.

(2) All mixtures of β , β^* , and β' (allowing for the most general case) produced by interrupting the premartensite transformation are: (a) metastable below the start temperature for the reverse premartensite transformation, and (b) remain metastable until recooled to approximately the interruption temperature. (3) Significant transformation occurs during isothermal holds in the premartensite transformation range. For example, analysis of the data presented in Figure 2 indicates that more than 70 percent of the β phase is transformed following the 30-minute hold at 39.1°C, while only ~ 30 percent is transformed with no isothermal hold. (4) The transformation remains incomplete for interruptions above approximately 38.9°C.

Figure 3 exhibits DSC curves for samples prepared in mixtures of phases as in Figure 2, with the cooling interrupted at 39.0°C, and then heated through the reverse premartensite ($\beta' \rightarrow \beta$) transformation temperature range. The results of these studies are completely in accord with observations (1) through (4) concerning the results of Figure 2. However, results of the type shown in Figure 3 exhibit a striking feature: the start temperature and initial reaction rate for the reverse premartensite transformation are independent of the fraction of β transformed and are identical to the values for 100 percent β' .

The results of the series of runs interrupting the premartensite transformation in $\text{Ni}_{50.5}\text{Ti}_{49.5}$ exemplified by the data in Figures 2 and 3 indicate that if T_r exists between T_i and T_f , then: (1) In contrast to the iron-doped NiTi case, the β' phase does not transform back to β^* on reheating. Evidence: no

energy is exchanged until the start temperature for the reverse premartensite transformation is reached nor is any transformation enthalpy unaccounted for. (2) The kinetics of the $\beta^* \rightarrow \beta$ and $\beta' \rightarrow \beta$ transformation are indistinguishable. This would be a truly remarkable finding since β^* is assumed to be a CDW state on the same cubic CsCl structure as in β , while β' corresponds to a rhombohedrally distorted CsCl phase. However, we cannot dismiss this possibility, because the SMW results in iron-doped NiTi indicate a remarkable similarity in the properties of β^* and β' . SMW provide evidence for continuous variation of electrical resistivity, specific heat, temperature derivative of magnetic susceptibility, and peak intensity of various superlattice reflections in the vicinity of T_r in 3.2 percent iron-doped NiTi, while the clear indication of the $\beta^* \rightarrow \beta'$ transformation is an abrupt, although subtle, splitting of certain Bragg peaks and the appearance of needle-like domains.

Nevertheless, it seems more plausible that if there is a temperature T_r in Ni_{50.5}Ti_{49.5}, it is extremely close to T_I making it impossible for us to interrupt transformation between T_I and T_r . Thus, a simpler explanation of the data in Figures 2 and 3 would be: (1) The breadth of the premartensite transformation reflects the fact that different regions of the sample transform from $\beta \rightarrow \beta'$ at slightly different temperatures. (2) The invariance of the start temperature and initial reaction rate with the amount transformed and the continuous variation of the form of the reverse premartensite transformation (as seen in Figure 3) imply that regions transform back to the β phase in reverse order to that in which they transform in the $\beta \rightarrow \beta'$ transformation. (3) Since only mixtures of β and β' are produced, there is no need to postulate that a third phase β^* exists that has identical metastability and transformation kinetics on heating and cooling to those of β' .

Mixtures of phases can also be prepared by partially transforming the β' phase by interrupting heating through the reverse premartensite transformation. DSC curves completely analogous to those of Figure 2 were obtained for appropriate thermal histories. For example, heating to 40.8°C, performing isothermal holds, cooling to 40°C, and finally, heating completely through the $\beta' \rightarrow \beta$ transformation yield peaks on the high side of the standard peak, and yield other effects analogous to those in Figure 2.

However, runs analogous to that shown in Figure 3 exhibit a new effect. The curves in Figure 4 were obtained by heating to 40.9°C, performing isothermal holds, and then cooling through the premartensite transformation ($\beta \rightarrow \beta'$) temperature range. Standard DSC curves are also shown. Figure 4 is typical of such interrupted reverse premartensite transformation runs. Apparently, the preexisting fraction of β' retained after partial transformation to β causes an increase in the start temperature and the initial reaction rate for the premartensite transformation. Note, however, that the start temperature and initial reaction rate are invariant to the specific amount of preexisting β' , as long as a detectable amount has been retained. Again, runs like that shown in Figure 4 yield a continuous set of curves, whose specific form is determined by the fraction transformed during the interrupted transformation. The simplest interpretation involves only two phases, β and β' , and is consistent with that given for interrupted premartensite transformations. The change in the start temperature and initial reaction rate in the case of retained β' could be attributed to the action of retained β' as nucleation sites for further transformations or sources of internal strains which then help drive the transformation. Interpretations in terms of a two-step transformation cannot be categorically rejected, although

one would have to interpret the variations of T_f and presumably, T_r , etc. with preexisting β' .

An interpretation of the facts in $\text{Ni}_{50.5}\text{Ti}_{49.5}$ in terms of pure phases with varying characteristics seems unlikely. For example, one would have to explain why the pure β' phase characterized by a given (metastable) rhombohedral angle would have its subsequent transformation properties determined by its immediate past history.

SUMMARY AND CONCLUSIONS

A DSC study of premartensitic effects in $\text{Ni}_{50.5}\text{Ti}_{49.5}$ has been performed. The thrust of the experimental effort was directed at determining ranges of metastability and transformation kinetics of the premartensitic phases and, in particular, to establish properties of the intermediate charge density wave phase identified by SMW in the closely related iron-doped NiTi alloys.

The premartensite transformation in $\text{Ni}_{50.5}\text{Ti}_{49.5}$ is quite sharp, having full width at half maximum (FWHM) $\approx 0.4^\circ\text{C}$ at $0.1^\circ\text{C}/\text{minute}$, compared to the corresponding transformations in iron-doped and stoichiometric NiTi. The transformation enthalpy is 4.75 J/g . Substantial isothermal transformation is observed for temperatures in the transformation range and a range of temperatures exists for which the transformation is incomplete for both the direct and reverse premartensite transformations. The direct and reverse transformation DSC peaks are separated by approximately 2°C .

Mixtures of phases or intermediate phases (for example, following SMW, β' phases with varying values of the rhombohedral angle) are metastable for temperatures ranging between approximately the temperature at which they are formed to the start temperature for the reverse transformation. Furthermore,

when such mixtures are brought through the reverse transformation, the start temperature and initial reaction rate are invariant. In the case of mixtures produced by interrupting the premartensite transformation $\beta \rightarrow \beta'$, the start temperature and initial reaction rate for the reverse premartensite transformation are identical to their values for 100 percent β' starting material. However, in the case of mixtures produced by interrupting the reverse premartensite transformation $\beta' \rightarrow \beta$, the start temperature and initial reaction rate for the premartensite transformation are larger than their value for 100 percent β starting material. All the DSC curves describing the subsequent behavior of mixtures of phases produced by interrupting the direct or reverse premartensite transformation fall into continuous sets governed only by the fraction transformed (independent of the temperature at which transformation occurs) with the exception of the 100 percent starting case.

If the premartensite transformation in $\text{Ni}_{50.5}\text{Ti}_{49.5}$ does consist of two separate phase transformations, then either (1) the temperature for the "lock-in" transformation T_L is very close to T_I , or (2) the metastability and reaction kinetics for phases β' and β^* are indistinguishable. The latter possibility cannot be dismissed because in the case of iron-doped NiTi , the β' and β^* phases have nearly identical physical properties, as may be seen in the continuity of specific heat, electrical resistivity, magnetic susceptibility, and a variety of superlattice reflection intensities at T_L in the work of SMW.

Nevertheless, it is more likely that a simpler interpretation involving only two phases, the CsCl structure β phase and the rhombohedrally distorted CsCl β' phase, is appropriate for $\text{Ni}_{50.5}\text{Ti}_{49.5}$. Data concerning ranges of metastability and reaction rates imply that the direct and reverse premartensite

transformation widths are due to a distribution of regions in the alloy, which transform from the cubic to the rhombohedrally distorted CsCl phase, $\beta \rightarrow \beta'$, over a range of temperatures. Then these regions transform back, $\beta' \rightarrow \beta$, in reverse order upon reheating. Data also support the hypothesis that the retained β' phase increases the start temperature and initial reaction for the premartensite transformation, $\beta \rightarrow \beta'$, while the retained phase has negligible effects on the $\beta' \rightarrow \beta$ transformation. This further suggests that the retained β' acts as nucleation sites for $\beta' \rightarrow \beta$.

The differences in premartensite behavior in the nickel-rich alloy, $\text{Ni}_{50.5}\text{Ti}_{49.5}$, and the iron-doped NiTi alloys, $\text{Ti}_{50}\text{Ni}_{47}\text{Fe}_3$ and $\text{Ti}_{50.1}\text{Ni}_{46.7}\text{Fe}_{3.2}$, are quite striking. Both types of alloys are interesting and commercially important in their own right. However, generalizations of behaviors observed in specific iron-doped or nonstoichiometric NiTi alloys may be unwise.

REFERENCES

1. C. Zener, Phys. Rev., Vol. 71, 1947, p. 846. However, this point is still subject to controversy; see, for example, P. Lindgard and O. G. Mouritsen, "Theory and Model for Martensitic Transformations," Phys. Rev. Lett., Vol. 57, No. 19, November 1986, pp. 2458-2461.
2. L. R. Testardi, "Structural Instability and Superconductivity in A-15 Compounds," Rev. Mod. Phys., Vol. 47, July 1975, p. 637.
3. B. W. Batterman and C. S. Barrett, "Crystal Structure of Superconducting V_3Si ," Phys. Rev. Lett., Vol. 13, 1964, p. 390 and "Low-Temperature Structural Transformation in V_3Si ," Phys. Rev., Vol. 145, 1966, p. 296.
4. N. Nakanishi, Shape Memory Effects in Alloys, (J. Perkins, ed.), Plenum, NY, 1975, p. 147.
5. L. Delaey, J. Van Paemel, and T. Struyve, "Relations Between the Premartensitic Instability of the Beta-Phase and the Martensite Structures and the Shape-Memory Effect in the Noble Metal Base Alloys," Scr. Metall., Vol. 6, June 1972, pp. 507-518.
6. G. D. Sandrock, A. J. Perkins, and R. F. Hehemann, "Premartensitic Instability in Near-Equiatomic Titanium," Metall. Trans., Vol. 2, October 1971, pp. 2769-2781.
7. M. Matsumoto and T. Honma, "Martensitic Transformation of Intermetallic Compound $Ti_{50}Ni_{47}Fe_3$," New Aspects of Martensitic Transformation, Japan Institute of Metals, Tokyo, 1976, pp. 199-204.
8. M. B. Salamon, M. F. Meichle, and C. M. Wayman, "Premartensitic Phases of $Ti_{50}Ni_{47}Fe_3$," Phys. Rev. B, Vol. 31, No. 11, June 1985, pp. 7306-7315.

9. R. V. Milligan, "Determination of Phase Transformation Temperatures of TiNi Using Differential Thermal Analysis," Titanium '80, Vol. 2, 1980, Kyoto, Japan.
10. K. Mukherjee, S. Sircar, and N. B. Dahotre, "Thermal Effects Associated With Stress-Induced Martensitic Transformation in a Ti-Ni Alloy," Mater. Sci. Eng., Vol. 74, September 1985, pp. 75-84.

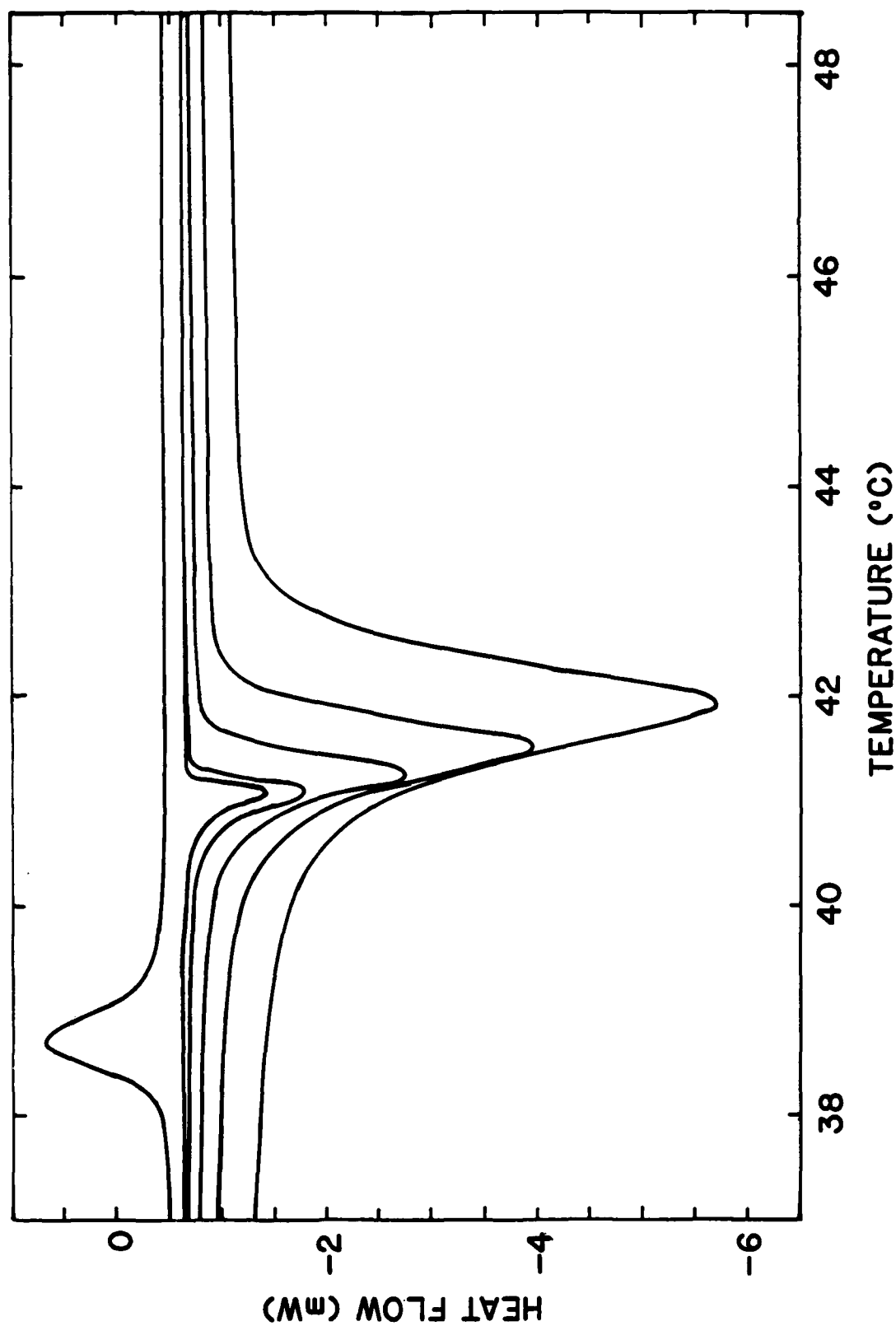


Figure 1. Heat flow versus temperature for constant heating rates of 0.1, 0.2, 0.5, 1.0, and 2.0°C/minute in Ni_{50.5}Ti_{49.5}. Also shown are four (essentially) identical cooling runs obtained for a rate of -0.5°C/minute made between the heating runs. These curves and those shown in the subsequent figures are uncalibrated; to obtain true heat flow multiply a given value by 0.86.

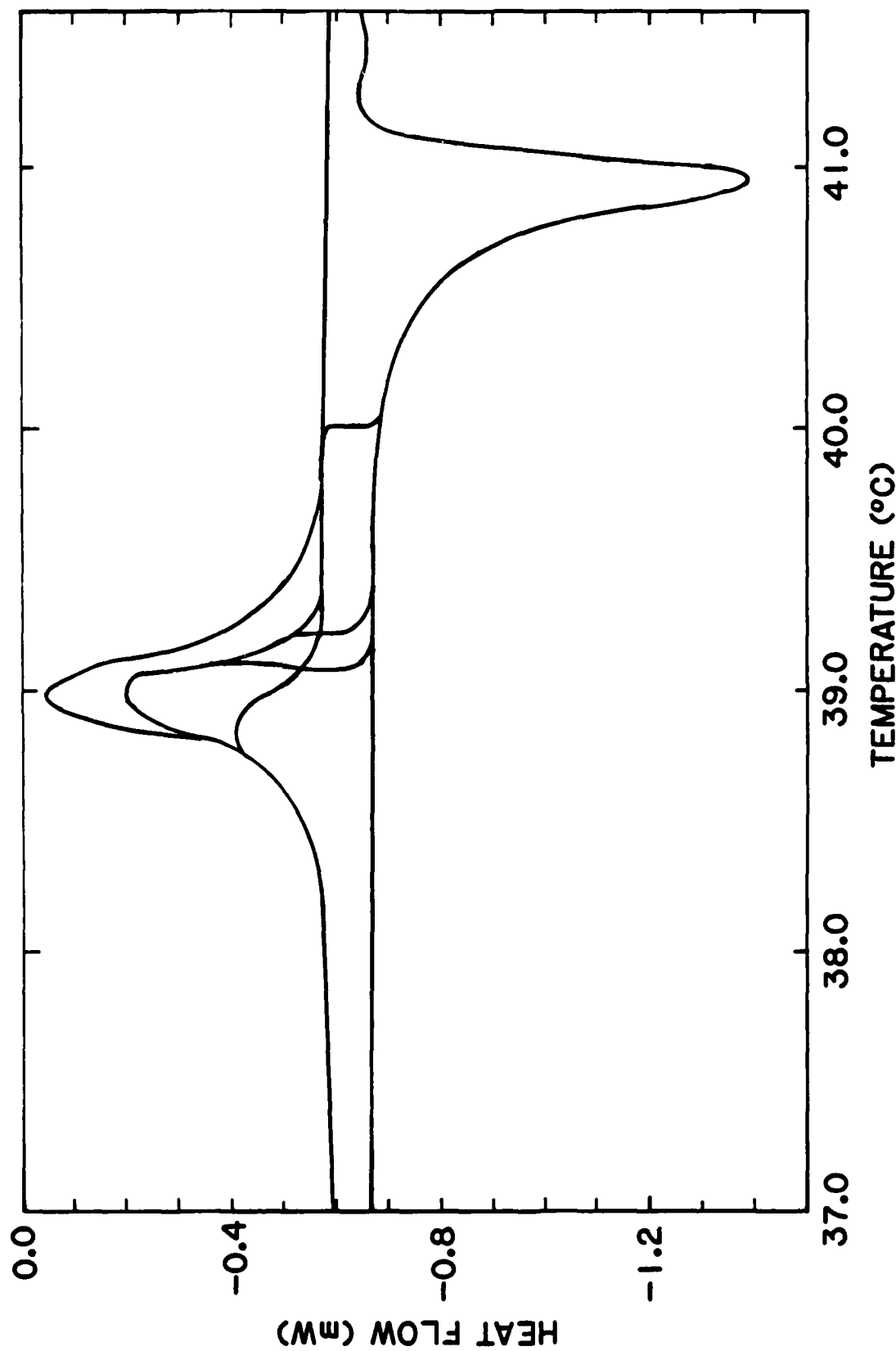


Figure 2. DSC results illustrating metastability and subsequent further transformation of mixtures of phases produced by interrupting the premartensite transformation in Ni_{50.5}Ti_{49.5}. Curves following 0 and 30-minute isothermal holds at 39.1°C are shown. Standard DSC curves are also shown. Heating and cooling rates were 0.1°C/minute. Isothermal holds greater than 8 minutes yield curves indistinguishable from the 30-minute case.

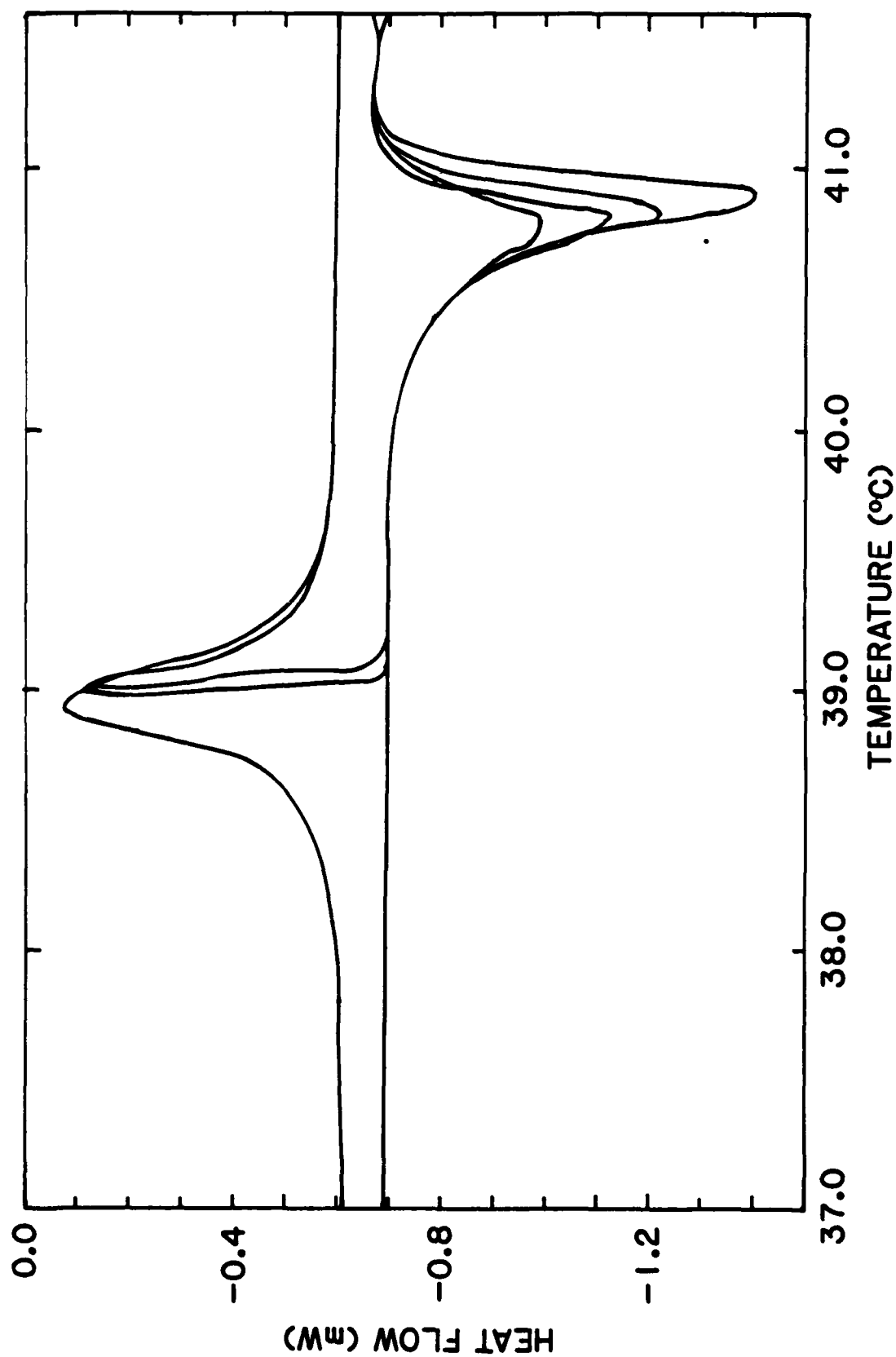


Figure 3. DSC results illustrating metastability and reverse transformation of mixtures of phases produced by interrupting the premartensite transformation in Ni_{50.5}Ti_{49.5}. Curves following 0, 2, and 30-minute isothermal holds at 39.0°C are shown. Standard DSC curves are also shown. Heating and cooling rates were 0.1°C/minute.

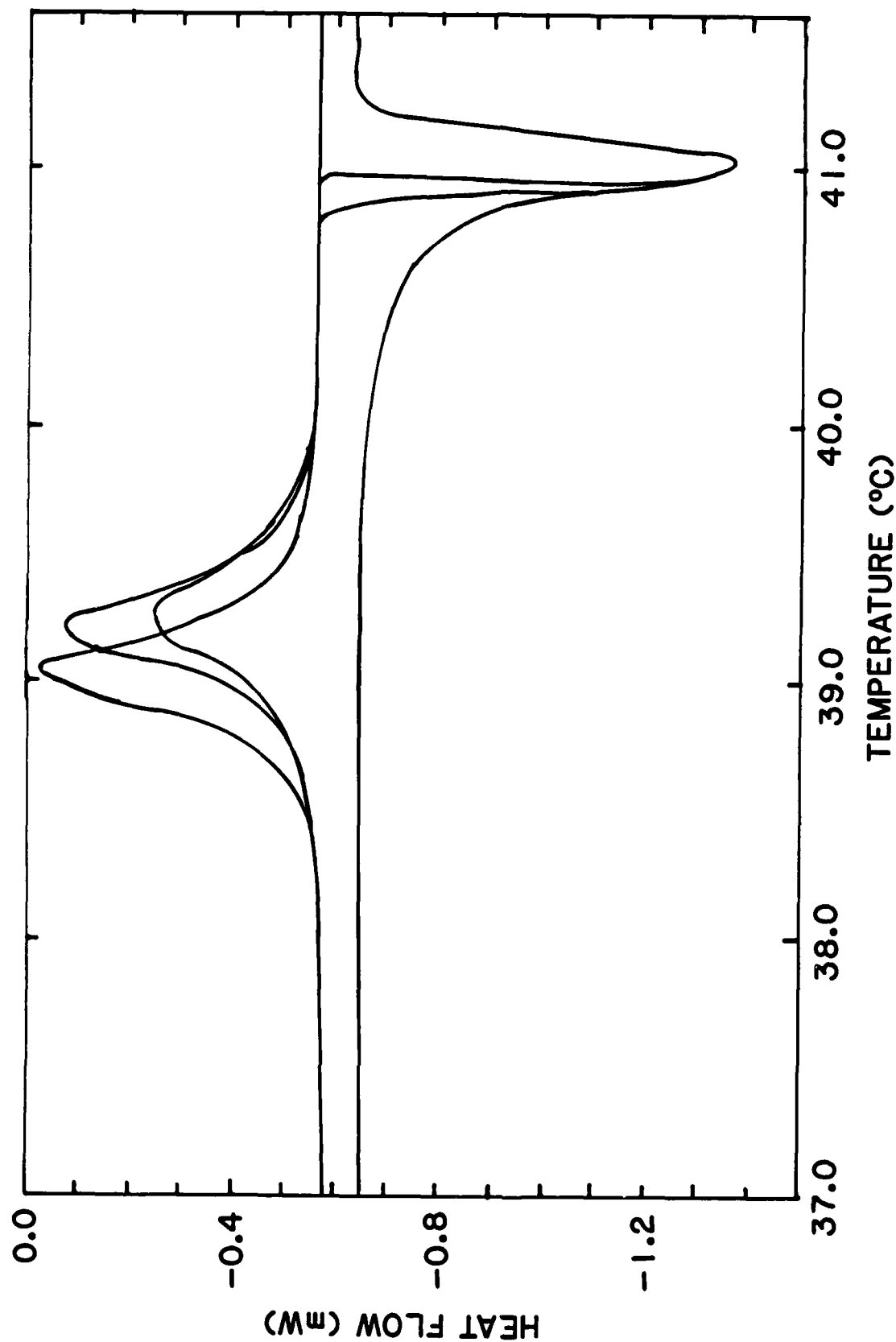


Figure 4. DSC results illustrating metastability and reverse transformation of mixtures of phases produced by interrupting the reverse premartensite transformation in $\text{Ni}_{50.5}\text{Ti}_{49.5}$. Curves following 0 and 30-minute isothermal holds at 40.9°C are shown. Standard DSC curves are also shown. Heating and cooling rates were 0.1°C/minute. Note the increased start temperature and initial reaction rate in the retained rhombohedrally distorted CsI phase cases.

TECHNICAL REPORT INTERNAL DISTRIBUTION LIST

	NO. OF COPIES
CHIEF, DEVELOPMENT ENGINEERING BRANCH	
ATTN: SMCAR-CCB-D	1
-DA	1
-DC	1
-DM	1
-DP	1
-DR	1
-DS (SYSTEMS)	1
CHIEF, ENGINEERING SUPPORT BRANCH	
ATTN: SMCAR-CCB-S	1
-SE	1
CHIEF, RESEARCH BRANCH	
ATTN: SMCAR-CCB-R	2
-R (ELLEN FOGARTY)	1
-RA	1
-RM	1
-RP	1
-RT	1
TECHNICAL LIBRARY	5
ATTN: SMCAR-CCB-TL	
TECHNICAL PUBLICATIONS & EDITING UNIT	2
ATTN: SMCAR-CCB-TL	
DIRECTOR, OPERATIONS DIRECTORATE	1
ATTN: SMCWV-OD	
DIRECTOR, PROCUREMENT DIRECTORATE	1
ATTN: SMCWV-PP	
DIRECTOR, PRODUCT ASSURANCE DIRECTORATE	1
ATTN: SMCWV-QA	

NOTE: PLEASE NOTIFY DIRECTOR, BENET LABORATORIES, ATTN: SMCAR-CCB-TL, OF ANY ADDRESS CHANGES.

TECHNICAL REPORT EXTERNAL DISTRIBUTION LIST

	<u>NO. OF COPIES</u>		<u>NO. OF COPIES</u>
ASST SEC OF THE ARMY RESEARCH AND DEVELOPMENT ATTN: DEPT FOR SCI AND TECH THE PENTAGON WASHINGTON, D.C. 20310-0103	1	COMMANDER ROCK ISLAND ARSENAL ATTN: SMCRI-ENM ROCK ISLAND, IL 61299-5000	1
ADMINISTRATOR DEFENSE TECHNICAL INFO CENTER ATTN: DTIC-FDAC CAMERON STATION ALEXANDRIA, VA 22304-6145	12	DIRECTOR US ARMY INDUSTRIAL BASE ENGR ACTV ATTN: AMXIB-P ROCK ISLAND, IL 61299-7260	1
COMMANDER US ARMY ARDEC ATTN: SMCAR-AEE	1	COMMANDER US ARMY TANK-AUTMV R&D COMMAND ATTN: AMSTA-DDL (TECH LIB) WARREN, MI 48397-5000	1
SMCAR-AES, BLDG. 321	1	COMMANDER US MILITARY ACADEMY ATTN: DEPARTMENT OF MECHANICS WEST POINT, NY 10996-1792	1
SMCAR-AET-O, BLDG. 351N	1		
SMCAR-CC	1		
SMCAR-CCP-A	1		
SMCAR-FSA	1		
SMCAR-FSM-E	1	US ARMY MISSILE COMMAND REDSTONE SCIENTIFIC INFO CTR ATTN: DOCUMENTS SECT, BLDG. 4484 REDSTONE ARSENAL, AL 35898-5241	2
SMCAR-FSS-D, BLDG. 94	1		
SMCAR-MSI (STINFO)	2		
PICATINNY ARSENAL, NJ 07806-5000			
DIRECTOR US ARMY BALLISTIC RESEARCH LABORATORY ATTN: SLCBR-DD-T, BLDG. 305 ABERDEEN PROVING GROUND, MD 21005-5066	1	COMMANDER US ARMY FGN SCIENCE AND TECH CTR ATTN: DRXST-SD 220 7TH STREET, N.E. CHARLOTTESVILLE, VA 22901	1
DIRECTOR US ARMY MATERIEL SYSTEMS ANALYSIS ACTV ATTN: AMXSY-MP ABERDEEN PROVING GROUND, MD 21005-5071	1	COMMANDER US ARMY LABCOM MATERIALS TECHNOLOGY LAB ATTN: SLCMT-IML (TECH LIB) WATERTOWN, MA 02172-0001	2
COMMANDER HQ, AMCCOM ATTN: AMSMC-IMP-L ROCK ISLAND, IL 61299-6000	1		

NOTE: PLEASE NOTIFY COMMANDER, ARMAMENT RESEARCH, DEVELOPMENT, AND ENGINEERING CENTER, US ARMY AMCCOM, ATTN: BENET LABORATORIES, SMCAR-CCB-TL, WATERVLIET, NY 12189-4050, OF ANY ADDRESS CHANGES.

TECHNICAL REPORT EXTERNAL DISTRIBUTION LIST (CONT'D)

	<u>NO. OF COPIES</u>		<u>NO. OF COPIES</u>
COMMANDER US ARMY LABCOM, ISA ATTN: SLCIS-IM-TL 2800 POWDER MILL ROAD ADELPHI, MD 20783-1145	1	COMMANDER AIR FORCE ARMAMENT LABORATORY ATTN: AFATL/MN EGLIN AFB, FL 32542-5434	1
COMMANDER US ARMY RESEARCH OFFICE ATTN: CHIEF, IPO P.O. BOX 12211 RESEARCH TRIANGLE PARK, NC 27709-2211	1	COMMANDER AIR FORCE ARMAMENT LABORATORY ATTN: AFATL/MNF EGLIN AFB, FL 32542-5434	1
DIRECTOR US NAVAL RESEARCH LAB ATTN: MATERIALS SCI & TECH DIVISION CODE 26-27 (DOC LIB) WASHINGTON, D.C. 20375	1 1	METALS AND CERAMICS INFO CTR BATTELLE COLUMBUS DIVISION 505 KING AVENUE COLUMBUS, OH 43201-2693	1

NOTE: PLEASE NOTIFY COMMANDER, ARMAMENT RESEARCH, DEVELOPMENT, AND ENGINEERING CENTER, US ARMY AMCCOM, ATTN: BENET LABORATORIES, SMCAR-CCB-TL, WATERVLIET, NY 12189-4050, OF ANY ADDRESS CHANGES.